Ultrabroadband photoconductive detection: Comparison with free-space electro-optic sampling

Shunsuke Kono, Masahiko Tani, and Kiyomi Sakai

Citation: Appl. Phys. Lett. **79**, 898 (2001); doi: 10.1063/1.1394719
View online: https://doi.org/10.1063/1.1394719
View Table of Contents: http://aip.scitation.org/toc/apl/79/7
Published by the American Institute of Physics

Ultrabroadband photoconductive detection: Comparison with free-space electro-optic sampling

Shunsuke Kono,[a] Masahiko Tani, and Kiyomi Sakai
Kansai Advanced Research Center, Communications Research Laboratory, 588-2, Iwaoka, Nishi-ku, Kobe 651-2492, Japan

(Received 13 February 2001; accepted for publication 18 June 2001)

The spectral response of a low-temperature-grown GaAs photoconductive (PC) antenna is compared with that of the electro-optic sampling technique for the frequency region up to 40 THz. The spectral response of the PC antenna for broadband detection is found to be determined by the temporal profile of the number of photocarriers injected by ultrashort optical gate pulses. © *2001 American Institute of Physics.* [DOI: 10.1063/1.1394719]

Photoconductive (PC) antennas gated with ultrashort optical pulses have been widely used and studied for the coherent detection of far-infrared electromagnetic transients called terahertz (THz) radiation. The response of the PC antenna was originally considered to be governed by the increase in photo-carrier number, however, their bandwidth has been reported to be up to several THz.[1,2]

We recently demonstrated that the PC antenna bandwidth can be extended about three times wider than the reported value by gating with optical pulses as short as 15 fs.[3] The achieved bandwidth of 20 THz[3] means that the bandwidth of the low-temperature-grown GaAs (LT–GaAs) PC antenna can be as broad as that of the electro-optic (EO) sampling technique using thin EO crystals for the coherent detection of THz radiation higher than 10 THz.[4,5]

This fast response of the PC antenna is explained by the rapid increase in the number of photocarriers injected by the ultrashort gating pulses. For ultrabroadband detection, the PC antenna works as an integrating detector, so the photocurrent from the antenna is supposed to be proportional to the time integration of the incident THz radiation.[6,7] In Ref. 3, we pointed out that the calculated time differentiation of the PC-detected THz wave form was similar to the EO-detected THz wave form. However, the differentiation of the wave forms assumes the temporal behavior of the number of photocarriers as a step function. Thus, further analysis has been necessary to quantitatively estimate the spectral response of the PC antenna for ultrabroadband detection.

In this letter, we experimentally compared the spectral response of a LT–GaAs PC antenna gated with 15 fs laser pulses with that of the EO sampling technique using a thin EO crystal, by measuring the THz radiation from the same ZnTe emitter. As a result, we found that the spectral response of the PC antenna is mainly determined by the temporal profile of the photocarrier number injected by the probe beam.

We used a mode-locked Ti:sapphire laser as the light source for the pump and probe measurements of THz radiation. We obtained a 12 fs pulse width at a 75 MHz repetition rate with an average power of 350 mW, a center wavelength of 800 nm, and a spectral width of 90 nm. The average pump-beam power was 120 mW after an optical chopper and that of the probe beam varied between 1 and 10 mW depending on the detectors.

The pulse width at the emitter and at the detectors was estimated to be about 15 fs by using a different cross-correlation measurement system. The pump beam was focused onto a 100-μm-thick (110) ZnTe crystal with a silver-coated off-axis parabolic mirror of 50 mm focal length to generate a broadband THz radiation by optical rectification effect. The generated THz beam was collimated by an off-axis parabolic mirror of 76 mm focal length and then focused onto the detectors by another identical parabolic mirror. The probe beam after the optical delay line was merged into the THz-radiation path by a high resistivity silicon wafer inserted between the two off-axis parabolic mirrors. Then the probe beam and THz radiation were made collinear and were focused at the same position on the detectors by the latter off-axis parabolic mirror. The detectors used were a dipole PC antenna or a 14-μm-thick (110) ZnTe crystal. They were carefully adjusted to the focal point of the THz radiation without changing the positions of other optical components.

The PC antenna was a 30 μm dipole photoconductive antenna with a 5 μm gap in the center. The metal electrodes were fabricated on 1.5-μm-thick LT–GaAs layer grown at 250 °C on a 0.4-mm-thick semi-insulating GaAs substrate. The carrier lifetime of the LT–GaAs was estimated to be 1.4 ps by measuring the transient photoreflectance. The antenna was reversed so that both the probe beam and THz radiation were incident on the side of the electrodes to avoid distortion of the wave form due to dispersion and absorption in the GaAs antenna substrate. This antenna geometry also enables replacing the PC antenna with the EO crystal without changing of the probe beam alignment and the THz radiation paths. The photocurrent from the PC antenna was preamplified with a low-noise current amplifier and then detected with a lock-in amplifier referenced to an optical chopper in the pump beam path. The total gain of the detection system was 10^{11} V/A.

For the EO detection, we used a 14-μm-thick (110) ZnTe crystal on a glass substrate. The p-polarized probe beam was directed into a quarter wave plate for a $\pi/2$-phase shift

[a]Present address: Fundamental Research Laboratory, NEC Corporation, 34 Miyukigaoka, Tsukuba-shi, 305-8501, Japan; electronic mail: s-kouno@cq.jp.nec.com

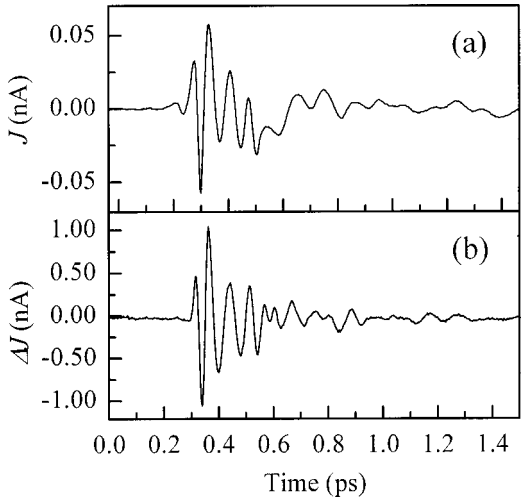

FIG. 1. (a) Time resolved wave form of THz radiation from (110) ZnTe emitter detected with PC antenna. (b) Time resolved wave form of THz radiation from (110) ZnTe emitter detected with EO sampling technique using 14-μm-thick (110) ZnTe crystal.

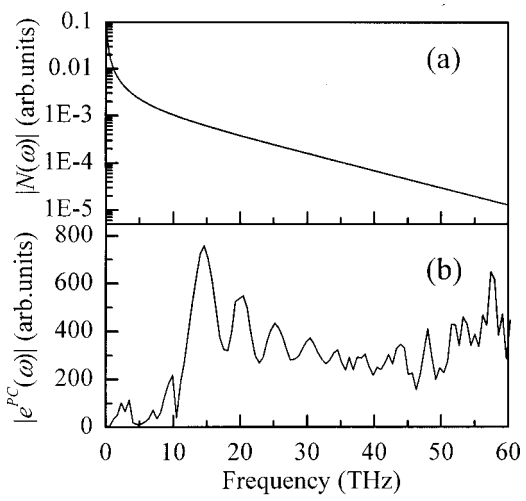

FIG. 3. (a) Frequency distribution of the photocarrier number in PC antenna injected by gating probe pulses. Solid curve represents $N(\omega)$ when the pulse width of the gating probe beam was 15 fs. (b) Fourier transformed spectrum shown in Fig. 2 divided by $N(\omega)$ when $\Delta t=15$ fs.

after passing through the thin EO crystal and then divided into s- and p-polarization components by a polarizing beam splitter. Both components were detected with an autobalanced photoreceiver, and the difference current was preamplified with a built-in preamplifier. The power of the probe beam was limited up to 1 mW to avoid saturation of the balanced receiver. The noise level of the measurement ($\Delta J/J_0$) was about 3.63×10^{-8} which was 44% above the shot noise limit ($J_0=0.257$ mA). After the lock-in amplification of the output voltage of the balanced photoreceiver, the total gain was 0.33×10^{10} V/A.

Figure 1(a) shows the signal wave form of the THz radiation from the (110) ZnTe emitter detected with the PC antenna. Very fast oscillations were observed and the shortest oscillation cycle was estimated to be 0.053 ps, which is about 25 times shorter than the carrier lifetime of the PC antenna. Figure 1(b) shows the signal wave form of the THz radiation from the same emitter detected by the EO sampling technique. The first four fast oscillation cycles are similar in the respective figures, but the subsequent slow oscillations differs from each other.

Figure 2 shows the Fourier transformed spectrum of the PC-detected signal THz wave form shown in Fig. 1(a). The frequency distribution of the detected radiation extends to about 50 THz. With the ZnTe emitter, the detectable bandwidth of the PC antenna was extended two times wider than the previous report.[3] The peaks at 14.3, 19.9, and 25.2 THz

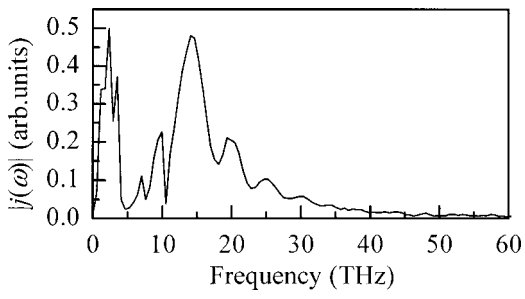

FIG. 2. Fourier transformed spectrum of the PC-detected signal wave form shown in Fig. 1(a).

are due to the phase-matching condition of the optical rectification effect in the ZnTe emitter. The absorption band around 5 THz is attributed to the TO phonon absorption ($\omega_{\mathrm{TO}}=5.3$ THz) in the ZnTe emitter.[8] The sharp absorption peak at 10.56 THz can be due to the two-phonon absorption of the TO phonon in the ZnTe emitter.

The photocurrent from the PC antenna, $J(t)$, is given by the following equation:[9]

$$J(\tau)=e\mu\int_{-\infty}^{\infty}E(t)N(t-\tau)dt,$$

where e is the electron charge and μ is the electron mobility. Here, $E(t)$ is the field amplitude of the THz radiation incident to the PC antenna and $N(t)$ is the number of photocarriers created by the gating probe beam. We suppose that $N(t)$ is determined by the increase in the number of carriers in the time of the full width at the half maximum of the gate pulse and by the decay of the carrier number determined by the carrier lifetime of the antenna substrate material. In this supposition, $N(t)$ is approximated by the following equation:

$$N(t)=N_0\exp(-t/\tau_c)[\tanh(1.76t/\Delta t)+1]/2,$$

where the carrier lifetime, τ_c, was 1.4 ps and the pulse width, Δt, was 15 fs. The solid curve in Fig. 3(a) shows the Fourier transformation of $N(t)$, represented by $N(\omega)$, with $\Delta t=15$ fs.

The frequency distribution of the photocurrent from the PC antenna, $j(\omega)$, is the frequency distribution of the incident THz radiation, $e(\omega)$, convoluted with $N(\omega)$:

$$|j(\omega)|\propto T_{\mathrm{GaAs}}(\omega)|e(\omega)||N(\omega)|.$$

Here, the Fresnel-transmission coefficient $T_{\mathrm{GaAs}}(\omega)=2/[1+n_{\mathrm{GaAs}}(\omega)]$ of the GaAs is included, and $n_{\mathrm{GaAs}}(\omega)$ is the refractive index of GaAs in the frequency range of THz.

Figure 3(b) shows the signal spectrum, $j(\omega)$, shown in Fig. 2 divided by $T_{\mathrm{GaAs}}(\omega)|N(\omega)|$. We denote this spectrum as $e^{\mathrm{PC}}(\omega)$. The spectral components lower than 10 THz are reduced while the higher ones are enhanced. The spectrum components higher than 40 THz are enhanced too much be-

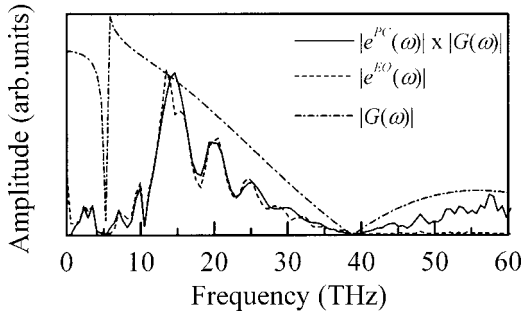

FIG. 4. Solid curve represents the Fourier transformed spectra shown in Fig. 3(b) multiplied by $G(\omega)$. Dashed curve represents the Fourier transformed spectrum of the EO-detected signal wave form shown in Fig. 1(b). Dotted-dashed curve represents $G(\omega)$.

cause the noise components of $j(\omega)$ are divided by $N(\omega)$, which rapidly decreases at high frequencies. The frequency components higher than 40 THz cannot be accurately reproduced in the present measurement conditions.

The dashed curve in Fig. 4 represents the Fourier transformed spectra of the EO-detected signal wave form shown in Fig. 1(b). We observed the structures as shown in Fig. 2 due to the group velocity mismatch and the phonon absorption lines in the ZnTe emitter. The spectral response of the EO sampling technique is explained by the frequency dependence of the mismatch between the group velocity of the gating probe beam and the THz phase velocity in the EO crystal, and by the reflection loss at the EO crystal surface, given by the following equation:[5]

$$G(\omega)=\frac{2}{n_{\mathrm{ZnTe}}(\omega)+1}\times\frac{c(\exp\{-i2\pi\omega d[n_g(\lambda_0)-n_{\mathrm{ZnTe}}(\omega)]/c\}-1)}{-i2\pi\omega d[n_g(\lambda_0)-n_{\mathrm{ZnTe}}(\omega)]},$$

where $n_g(\lambda_0)$ is the group refractive index of the probe beam calculated from the refractive index of ZnTe in the near-infrared region[10] and $n_{\mathrm{ZnTe}}(\omega)$ is the refractive index of ZnTe from the far to midinfrared region.[11] The crystal thickness, d, was 14 μm. The dashed-dotted curve in Fig. 4 shows the estimation of $G(\omega)$. The cutoff observed at 39 THz was consistent with the estimation using the above formula, where $G(\omega)=0$.

As $e^{\mathrm{PC}}(\omega)$ is considered to be the actual spectrum of the THz radiation incident on the detectors, we expected $e^{\mathrm{PC}}(\omega)$ filtered by $G(\omega)$ to reproduce the spectrum of the THz radiation detected with the EO sampling technique. The solid curve in Fig. 4 shows the spectrum $e^{\mathrm{PC}}(\omega)$ multiplied by $G(\omega)$, which well reproduces up to 40 THz the EO-detected Fourier transformed spectrum represented by the dashed curve. The signal higher than 40 THz in the solid curve is an artifact due to the division by $N(\omega)$. This comparison shows that the spectral distribution of the PC antenna is mainly determined by the temporal profile of the number of the electrons injected by the ultrashort-gate optical pulses.

Our comparison shows that the PC-antenna frequency response seems independent on its geometrical structure. We did not clearly observe the resonant peaks due to the antenna structure. This may be due to the large radiation loss on the antenna structure, especially in the frequency range higher than several THz. Thus, the characteristic impedance of the antenna does not show a strong frequency dependence.[12] Besides the radiation impedance, the antenna structure affects the collection efficiency of the incident radiation. This efficiency is determined by the overlap between the focal spot of the THz beam and PC antenna dipole. As the THz beam spot size depends on the frequency, the collection efficiency also depends on the frequency of the incident radiation.[13] The focal size of the gating probe beam at the detectors was estimated to be about 30 μm. The area on the EO crystal sensitive to the incident radiation was defined by the probe beam size and was comparable to the PC-antenna size (30 μm). In our detection geometry, the relative position and overlapping between the THz beam and gating probe beam were the same for both the detectors. Therefore, the size effect for both the detectors was the same and will not affect the comparison of the spectral response in terms of the THz collection efficiency. More detailed analysis on the antenna effect will be discussed in another paper.

In conclusion, we compared the spectral response of a PC antenna gated with 15 fs laser pulses with that of the EO sampling technique using a thin EO crystal. After the correction considering the temporal profile of the photocreated carriers and the group velocity mismatch in the EO detection, the Fourier transformed spectrum obtained by the PC antenna reproduced the one obtained by the EO sampling technique. This comparison shows that the spectral response of the PC antenna for broadband detection is mainly determined by the temporal behavior of the number of photocreated carriers.

The authors thank Hironori Takahashi at Hamamatsu Photonics K. K. for providing the thin ZnTe crystals.

[1] S. E. Ralph, S. Perkowitz, N. Katzennellenbogen, and D. Grischkowsky, J. Opt. Soc. Am. B **11**, 2528 (1994).
[2] P. Gu, M. Tani, K. Sakai, and T.-R. Yang, Appl. Phys. Lett. **77**, 1798 (2000).
[3] S. Kono, M. Tani, P. Gu, and K. Sakai, Appl. Phys. Lett. **77**, 4104 (2000).
[4] Q. Wu and X.-C Zhang, Appl. Phys. Lett. **71**, 1285 (1997).
[5] A. Leitenstorfer, S. Hunsche, J. Shah, M. C. Nuss, and W. H. Knox, Appl. Phys. Lett. **74**, 1516 (1999).
[6] F. G. Sun, G. A. Wagoner, and X.-C. Zhang, Appl. Phys. Lett. **67**, 1656 (1995).
[7] M. Tani, K. Sakai, and H. Mimura, Jpn. J. Appl. Phys., Part 2 **36**, L1175 (1997).
[8] O. Madelung, *Semiconductor—Basic Data*, 2nd edition (Springer, Berling, 1996).
[9] S.-G. Park, M. R. Melloch, and A. M. Weiner, Appl. Phys. Lett. **73**, 3184 (1998).
[10] D. Palik, *Handbook of Optical Constants of Solids* (Academic, San Diego, 1998).
[11] A. Manabe, A. Mitsuishi, and H. Yoshinaga, Jpn. J. Appl. Phys. **6**, 593 (1967).
[12] P. R. Smith, D. H. Auston, and M. C. Nuss, IEEE J. Quantum Electron. **24**, 255 (1988).
[13] P. Uhd Jepsen, R. H. Jacobsen, and S. R. Keiding, J. Opt. Soc. Am. B **13**, 2424 (1996).